

DEC 23 1946

ARR Mar. 1943

NATIONAL ADVISORY COMMITTEE FOR AERONAUTICS

WARTIME REPORT

ORIGINALLY ISSUED

March 1943 as
Advance Restricted Report

AN INVESTIGATION OF AIRCRAFT HEATERS
VIII - A SIMPLIFIED METHOD FOR THE CALCULATION OF
THE UNIT THERMAL CONDUCTANCE OVER WINGS

By R. C. Martinelli, A. G. Guibert,
E. H. Morrin, and L. M. K. Boelter
University of California

NACA

WASHINGTON

NACA LIBRARY
LANGLEY MEMORIAL AERONAUTICAL
LABORATORY
Langley Field, Va.

NACA WARTIME REPORTS are reprints of papers originally issued to provide rapid distribution of advance research results to an authorized group requiring them for the war effort. They were previously held under a security status but are now unclassified. Some of these reports were not technically edited. All have been reproduced without change in order to expedite general distribution.

NATIONAL ADVISORY COMMITTEE FOR AERONAUTICS

ADVANCE RESTRICTED REPORT

AN INVESTIGATION OF AIRCRAFT HEATERS

VIII - A SIMPLIFIED METHOD FOR THE CALCULATION OF
THE UNIT THERMAL CONDUCTANCE OVER WINGS

By H. G. Martinelli, A. G. Guibert,
E. H. Morrin, and L. M. K. Boelter

SUMMARY

A simplified approximate method of calculating the unit thermal conductance along an airfoil as a function of distance from the leading edge, by use of heat transfer data for smooth cylinders and smooth flat plates, is presented. Heat transfer rates experimentally obtained by several investigators on models of airfoils of sections R.A.F. 26, R.A.F. 30, Clark Y, and NACA M-6 are compared with results predicted by the use of this method. Calculations of the heat transfer rates to be expected from a typical full-scale wing are also given.

INTRODUCTION

The design of an effective system for the distribution of heat over wing surfaces to prevent the formation of ice requires a knowledge of the unit thermal conductances along such surfaces.

In order to utilize existing heat-transfer data to calculate these unit conductances, the following ideal system is defined: The leading edge of the airfoil is replaced by a right circular cylinder with a radius approximately equal to the radius of curvature of the leading edge and the upper and the lower surfaces of the airfoil are replaced by smooth flat plates. The mechanism of heat transfer along the leading edge of the airfoil then corresponds to that existing over smooth right circular cylinders, and the mechanism along the remainder of the airfoil is postulated to be equivalent to that existing over smooth flat plates.

SYMBOLS

A	area of airfoil equal to chord times span, ft^2
C_p	unit heat capacity of the fluid at constant pressure, $\text{Btu/lb } ^\circ\text{F}$
C_L	lift coefficient defined in $F_L = \frac{1}{2} C_L \rho A u_\infty^2$ (dimensionless)
d	diameter of cylinder, ft
f_c	average unit thermal convective conductance, for length L , between airfoil surface and air, $\text{Btu/hr ft}^2 ^\circ\text{F}$
f_{c_x}	unit thermal convective conductance between airfoil surface and air at any point x , $\text{Btu/hr ft}^2 ^\circ\text{F}$
f_{c_ϕ}	unit thermal convective conductance between airfoil surface and air at any angle ϕ , $\text{Btu/hr ft}^2 ^\circ\text{F}$
$f_{c_{\phi=0}}$	unit thermal convective conductance between airfoil surface and air at stagnation point ($\phi=0^\circ$), $\text{Btu/hr ft}^2 ^\circ\text{F}$
F_L	lift force defined by $F_L = \frac{1}{2} C_L \rho A u_\infty^2$, lb
g	gravitational force per unit mass, $\text{lb}/(\text{lb sec}^2/\text{ft})$
k	thermal conductivity of fluid, $\text{Btu/hr ft}^2 (^\circ\text{F}/\text{ft})$
L	length of flat plate equivalent to length along airfoil surface measured from point of stagnation, ft
n	exponent of L in equations (5) and (7) (dimensionless)
q	rate of heat transfer, Btu/hr
b	width of span, ft
t_s	temperature of airfoil surface, $^\circ\text{F}$
T	arithmetic average absolute temperature of fluid and airfoil surface, $^\circ\text{R}$

u_m	velocity of fluid defined by equation (12) or from pressure distribution, ft/sec
u_∞	free-stream velocity of fluid, ft/sec
x	length along airfoil profile measured from the point of stagnation, ft
x_{trans}	length along airfoil profile measured from point of stagnation to point of the beginning of transition of boundary layer, ft
x_u	length along upper surface of airfoil measured from point of stagnation, ft
x_L	length along lower surface of airfoil measured from point of stagnation, ft
α	angle of attack of airfoil, degrees
γ	weight density of fluid at temperature T , lb/ft ³
μ	absolute viscosity of fluid at temperature T , lb sec/ft ²
ρ	mass density of fluid at temperature T , lb sec ² /ft ⁴
T_∞	uniform temperature of fluid far from airfoil surface, °F
ϕ	angle between radius through point on cylinder and radius through point of stagnation measured at axis of cylinder, degrees
Nu	Nusselt number ($f_c d/k$)
Pr	Prandtl number ($3600\mu C_p g/k$)
Re	Reynolds number ($u_\infty \gamma / \mu g$) (applicable to cylinders)
Re_x	Reynolds number at distance x from stagnation point ($u_\infty \gamma x / \mu g$)
Re_{trans}	Reynolds number at point of beginning of transition of boundary layer ($u_\infty \gamma x_{trans} / \mu g$)

DISCUSSION OF METHOD

Leading Edge

The magnitude of the unit thermal conductance at the stagnation point of a cylinder can be expressed (reference 1, vol II, p. 632) as

$$Nu = 1.14 Pr^{0.4} Re^{0.50} \quad (1)$$

where

$$Nu = \frac{f_c d}{k}$$

$$Pr = 3600 \frac{\mu C_p g}{k}$$

$$Re = \frac{u_\infty d \gamma}{\mu g}$$

The variation of the unit conductance along the forward half of a smooth cylinder may be obtained from the data of Schmidt and Wenner (reference 2). On the basis of these data the unit conductance at any angle φ , measured from a radius through the point of stagnation--that is, at $\varphi = 0^\circ$ --can be expressed approximately as a function of the unit conductance at the point of stagnation for $0^\circ \leq \varphi \leq 90^\circ$. Inspection of these data (reference 2) reveals that as a fair approximation

$$f_{c\varphi} = f_{c\varphi=0^\circ} \left(1 - \left|\frac{\varphi}{90}\right|^3\right) \quad (2)$$

This expression may be utilized to calculate the unit conductance along the cylinder, which represents the leading edge of the airfoil in the ideal system under consideration.

Combining equations (1) and (2) gives

$$\frac{f_{c\varphi} d}{k} = 1.14 \text{Pr}^{0.4} \text{Re}^{0.50} \left(1 - \left|\frac{\varphi}{90}\right|^3\right) \quad (3)$$

Thus

$$f_{c\varphi} = 21.2 \left(\mu^{-0.1} c_p^{0.4} k^{0.6}\right) \left(\frac{u_\infty \gamma}{d}\right)^{0.50} \left(1 - \left|\frac{\varphi}{90}\right|^3\right)$$

Since the term $\mu^{-0.1} c_p^{0.4} k^{0.6}$ for air can be expressed approximately as a power function of the absolute temperature T , the equation for f_c becomes, for $0^\circ \leq \varphi \leq 90^\circ$,

$$f_{c\varphi} = 0.194 T^{0.49} \left(\frac{u_\infty \gamma}{d}\right)^{0.50} \left(1 - \left|\frac{\varphi}{90}\right|^3\right) \quad (4)$$

where

d diameter of cylinder

u_∞ free-stream velocity

γ weight density at temperature T

and

T arithmetic average of temperatures of free stream and of airfoil surfaces

Airfoil Surfaces

The average unit conductance, with length, along a flat plate of length L is calculated from the equations of Colburn (reference 3, which are used in reference 4).

For the laminar regime,

$$\frac{f_c}{3600 u_m \gamma c_p} \text{Pr}^{2/3} = 0.66 \left(\frac{u_m L \gamma}{\mu g}\right)^{0.50} \quad (5)$$

or

$$f_c = 5.67 \left(k^{0.667} \mu^{-0.167} C_p^{0.333} \right) \left(\frac{u_m \gamma}{L} \right)^{0.50}$$

Again the properties of air may be expressed approximately in terms of the absolute temperature T . Then,

$$f_c = 0.113 T^{0.50} \left(\frac{u_m \gamma}{L} \right)^{0.50} \quad (6)$$

For the turbulent regime,

$$\frac{f_c}{0.660 u_m \gamma C_p} Pr^{2/3} = 0.037 \left(\frac{u_m L \gamma}{\mu g} \right)^{-0.20} \quad (7)$$

The coefficient 0.037 found in references 3 and 4, which is the constant that relates the drag coefficient and Reynolds number, has been changed to agree with that of Goldstein, 0.074/2 (fig. 110, vol. II, pp. 366 and 367 of reference 1).

As

$$f_c = 0.109 \left(k^{0.667} \mu^{-0.467} C_p^{+0.333} \right) \left(\frac{u_m \gamma}{L^{0.25}} \right)^{0.50}$$

then

$$f_c = 0.655 T^{0.256} \left(\frac{u_m \gamma}{L^{0.25}} \right)^{0.50} \quad (8)$$

The unit conductance at any point x along the flat plate is related to the average unit conductance over the total length L by the equation

$$f_{cx} = f_c (n+1) \quad (9)$$

where f_c is the average conductance for the length x from equation (8), and n is the exponent of L in equations (5) and (7) (reference 4). The unit conductance along the flat plate, which in the ideal system is equivalent to the portion of the profile beyond the leading edge, may be expressed by

$$f_{c_x} = 0.0562 T^{0.50} \left(\frac{u_m \gamma}{x} \right)^{0.50} \quad (10)$$

for the laminar regime, and by

$$f_{c_x} = 0.524 T^{0.298} \left(\frac{u_m \gamma}{x^{0.25}} \right)^{0.50} \quad (11)$$

for the turbulent regime

where x is the distance along the flat plate measured from the point of stagnation of the airfoil. The unit thermal conductance f_{c_x} as a function of $u_m \gamma/x$ and of $u_m \gamma/x^{0.25}$ for use in equations (10) and (11), respectively, is shown in figure 1.

Because of the circulation around the actual airfoil, the velocity of the fluid is greater along the upper surface and smaller along the lower surface than the free-stream velocity u_∞ . In reference 5 it is demonstrated that, as a first approximation, the velocity to be used in equations (10) and (11) for the lower and upper surfaces of the airfoil is

$$u_m = u_\infty \left(1 \pm \frac{C_L}{4 \cos \alpha} \right) \quad (12)$$

in which C_L is the lift coefficient of the airfoil defined by $F_L = \frac{1}{2} C_L \rho A u_\infty^2$ and α is the angle of attack. The positive sign in equation (12) is used in the computation of the velocity along the upper surface and the negative sign is used for the velocity along the lower

surface. The velocity distribution derived from pressure measurements along the airfoil may also be used for the evaluation of u_m in equations (10) and (11). This procedure yields slightly higher values of f_{cx} near the leading edge on the upper surface but the average unit conductance, with length, does not differ greatly from that obtained from equation (12). The value of f_{cx} on the lower surface, where the flow is usually laminar over a large part of the airfoil, is not so greatly influenced by the magnitude of u_m which enters into equation (10) as the 0.50 power.

Transition between Laminar and Turbulent Boundary Layer

In order to calculate the unit conductance of an actual airfoil at a given angle of attack α , an equivalent cylinder is substituted for the leading edge and the local unit conductance is computed up to an angle of $\pm 90^\circ$ by use of equation (4) and the free-stream velocity u_∞ . The variation of the position of the stagnation point with the angle of attack is neglected in this calculation because its change of position is small compared to the chord of the airfoil.

The unit conductance for the portion of the airfoil following the equivalent cylinder is calculated from the flat-plate equations (10) and (11), by using the distance along the profile measured from the point of stagnation x and the corrected velocity u_m . The value of the absolute temperature T in equations (4), (10), and (11) is defined as the arithmetic mean of the fluid and the airfoil temperatures.

An examination of equation (10) indicates that, for the region of laminar flow, the magnitude of f_{cx} actually is independent of the arithmetic mean absolute temperature T . This result is due to the fact that the properties of air $k 0.887 \mu^{-0.167} C_p 0.333$ are proportional to the 0.50 power of T while the weight density γ , which is inversely proportional to the absolute temperature T , enters with the 0.50 power in equation (6). The magnitude of f_{cx} in equation (4) is practically independent of T , since the properties of air - that is, k , μ , and C_p - are a function of the 0.49 power of T . For the region of turbulent flow (equation (11)), a similar procedure reveals that the local unit convective conductance is proportional to the -0.50 power of T .

An approximate picture of the flow conditions in the boundary layer along a flat plate is shown in figure 3 of reference 6.

The point of transition of the boundary layer from laminar flow to turbulence is indeterminate. The position of this point is a function of the free-stream velocity and the corresponding turbulence, the angle of attack, the shape of the airfoil, the surface roughness, and other variables. The point of transition along the upper surface may be estimated roughly, however, by setting $Re_{trans} = \frac{u_m x_{trans}}{\mu g}$

(reference 1, vol I, p. 326) equal to a value between 5×10^4 and 5×10^5 . These magnitudes of Re_{trans} refer to the point at which turbulence begins. The rate at which turbulent flow becomes fully developed may be estimated from the behavior of the experimental values of f_{cx} . The position of the point of transition along the lower surface is also unknown, although some evidence indicates that the boundary layer along the lower surface of models is laminar for a considerable part of the chord at angles of attack greater than 0° .

Rate of Heat Transfer from Airfoil

Figure 2 illustrates the distribution of the point unit thermal conductance f_{cx} obtained by the method previously outlined. The lower surface would have a distribution similar to that shown along the upper surface but would yield somewhat lower magnitudes of f_{cx} because of lower values of u_m , and the transition point would occur at a greater distance from the leading edge.

The maximum average unit conductance over the whole airfoil occurs when the point of transition is close to the nose. As a conservative estimate, the heating system should be designed for this position of the transition point, since any disturbance, such as initial ice formation, would tend to move the transition point forward.

The rate of heat transfer from the whole airfoil may be calculated by the equation

$$q = \int_0^{x_u} f_{cx} (t_s - t_\infty)_x b \, dx + \int_0^{x_l} f_{cx} (t_s - t_\infty)_x b \, dx \quad (13)$$

where

b span

x_u heated length, measured along profile on upper surface

x_L heated length, measured along profile on lower surface

$(t_s - t_\infty)_x$ difference in temperature between airfoil surface and ambient fluid at point x measured from leading edge.

DISCUSSION OF EXPERIMENTAL DATA

R.A.F. 26 Model

Observations of the thermal characteristics of an R.A.F. 26 airfoil (reference 7) are given in figure 3, which also shows the predicted values of f_{cx} as a function of the distance x along the profile. The tests were performed on a 6-inch airfoil model, which was heated electrically by means of platinum resistance strips placed spanwise on both upper and lower surfaces.

The predicted unit conductances for the nose were set equal, as proposed herein, to the unit conductances along a cylinder having a radius equivalent to the radius of curvature of the leading edge. The variation of the unit conductance with distance along the upper and lower surfaces was then obtained from equations (10) and (11) by using the corrected velocities u_m .

The experimental result for the unit conductance at the nose is always lower than the predicted value at the point of stagnation because the measured value is an average over a heated strip which includes more surface than the point of stagnation. The position of this point is a function of the angle of attack, but the predicted values are based on a point of stagnation fixed at the leading edge.

On the lower surface of the airfoil at $\alpha = -0.9^\circ$ (fig. 3), the experimental results can be predicted for a given position of the transition point. The experimental data indicate that this point moves toward the leading edge

as the free-stream velocity is increased. At $\alpha = 3.2^\circ$ (fig. 4), the flow is apparently laminar along most of the length of the surface and the unit conductance can be closely predicted. The agreement of predicted and experimental results becomes better as the velocity u_∞ is decreased and as the angle of attack α is increased, because the laminar layer is more stable at small magnitudes of u_m . Owing to the circulation around the airfoil, the local velocity u_m , calculated from equation (12), is less than the free-stream velocity u_∞ and decreases as α increases. The predicted results for the lower surface are inappreciably affected by the use of the tabulated values of the fluid velocity just outside the boundary layer.

Along the upper surface also the unit conductance can be predicted if the transition point is known. As might be expected, the experimental results for $\alpha = -0.9^\circ$ show that the transition point occurs far back along the trailing edge of the 6-inch model and that it moves forward as u_∞ increases. For $\alpha = 3.2^\circ$ and $\alpha = 7^\circ$ (figs. 4 and 5), the calculations for the ideal system do not predict the very high values of the unit conductances that apparently occur in the region of transition from laminar to turbulent flow. This deviation between the predicted and the experimental results could be made smaller if the distance along the equivalent flat plate x were measured, not from the point of stagnation, but from some point farther back along the plate. The deviation may be ascribed to the great curvature of the airfoil in the region of the leading edge, which may invalidate substitution of a flat plate for the airfoil in that region, and the use of u_m . The change in x would not appreciably affect the predicted results along the rear half of the chord but would have a great effect upon the slope within the first 30 percent of the chord, since f_{cx} varies as $x^{-0.2}$. The slopes of the theoretical curves of f_{cx} against x approach small and almost constant magnitudes with increasing values of x . The experimental values along the upper surface rapidly diminish at the trailing edge; the experimental values along the lower surface rapidly rise and, at the end of the model airfoil, approach the same value as those along the upper surface. The previously mentioned deviations between the predicted and the experimental results near the region of transition can also be made smaller (fig. 4(c)) if the tabulated velocity distribution is used in equations (10) and (11) instead of the value of u_m derived from equation (12). This method,

however, does not predict the very high value of the unit conductance which occurs at the point where the boundary layer is apparently fully turbulent. The corresponding result near the trailing edge is the same as that when the value of u_m from equation (12) is used.

R.A.F. 30 Model

The experimental results on a 24-inch model of an R.A.F. 30 airfoil at $\alpha = 5.3^\circ$ are compared with predicted values in figure 6. The heated surface, located at the nose, comprised approximately 25 percent of the chord for the upper surface and 14 percent of the chord for the lower surface. The total heat loss of the entire heated surface was determined in the experimental work (reference 8) for several angles of attack at velocities ranging from 40 feet per second to 130 feet per second.

The predicted variation of the unit conductance was determined according to the methods proposed herein, after arbitrarily locating the point of transition at which turbulence begins. For the upper surface this point was taken at different velocities for Re_{trans} from 20,000 to 300,000, which corresponded in each case to transition at a point close to the nose. For the lower surface these points of transition were taken at Re_{trans} from 30,000 to 400,000. These predicted values of the unit conductances were averaged with respect to distance along the airfoil over the entire length of the heated section (both upper and lower surfaces) for each velocity. The averaged predicted values are about 20 percent lower at all velocities when u_m was determined from equation (12) and about 10 percent lower when the velocity distribution derived from pressure measurements along the airfoil was used for the values of u_m than the corresponding experimental results.

Clark Y Model

The data for a Clark Y airfoil were taken on a 10-inch model (reference 9), which was heated in four separate sections along the chord, including the leading and the trailing edges. The predicted values were determined for one velocity and for two different angles of attack. Data and predicted values are compared in figure 7. The predicted unit conductance over the upper and lower surfaces included points of transition for which the values of the Reynolds number were 2.3×10^4 at $\alpha = 6^\circ$ and 3.2×10^4 at $\alpha = 0^\circ$ for the upper surface and 1.5×10^5 at $\alpha = 6^\circ$ and 1.3×10^5

at $\alpha = 0^\circ$ for the lower surface. The predicted values again appeared to be, at the most, about 20 percent lower than the experimental results averaged with respect to length for each section. The values of u_m were calculated from equation (12).

NACA M-6 Model

Experimental data taken on a 10-inch model of an NACA M-6 airfoil (reference 10) are presented in figure 8 for $\alpha = 4^\circ$ and for free-stream velocities ranging from 98 feet per second to 203 feet per second. The model was heated at the nose and at three contiguous sections on the upper surface and on the lower surface. The heat transfer from each heated section was determined and is shown in figure 8 as constant values over each section. The experimentally determined conductances are superposed upon the predicted distribution of conductance along the airfoil. If the flow over the entire model were considered to be laminar along most of the lower surface, the experimental results could be predicted closely. The measured values of the conductance along the upper surface clearly indicate the increase in the value of f_{cx} when the boundary layer becomes turbulent. Values for the unit conductance for the case when the nose section was not heated are also shown in figures 8(b) and 8(d). The fact that the heat transfer from the other sections is higher when the nose is not heated may be explained by a delayed transition of the boundary layer from laminar to turbulent flow due to the removal of the initial disturbance; that is, the heated nose section.

It should be kept clearly in mind that, for a model, the distribution of the conductance depends a great deal on the position of the transition point; but, in the case of a full-size airfoil, the transition region is a small part of the total area usually heated and for this reason its position need not be accurately known.

NUMERICAL EXAMPLE

As a further illustration of the application of the proposed method for computation of the distribution of the unit conductance along a full-size airfoil, an example is presented.

The distribution of the unit conductance along an actual airfoil with a 6-foot chord and a profile which approximates that of the NACA 23012 is shown in figure 9 for $\alpha = 0^\circ$ and for a free-stream velocity equal to 440 feet per second (300 mph). The transition point for the beginning of turbulence for these conductances was taken at a value of Re_{trans} of approximately 0, which is at the stagnation point, and at 500,000.

If the airfoil were heated for a distance of 2 feet along both the upper and the lower surfaces, the predicted average unit conductance for this section, when values of u_m calculated from equation (12) are used, would be only 10 percent lower at a free-stream velocity of 300 miles per hour and 23 percent lower at a free-stream velocity of 150 miles per hour (see fig. 9), when Re_{trans} is taken to be 500,000 than the unit conductance when Re_{trans} is at the leading edge - that is, when $Re_{trans} = 0$.

These calculations demonstrate the fact that for a full-size airfoil the exact position of the transition point becomes less important at higher velocities and for larger heating sections, since a great variation in the position of this point was arbitrarily chosen - that is, Re_{trans} at 0 and at 500,000.

The distribution of the unit conductance when the value of u_m is taken from pressure measurements along the airfoil is also shown in figure 9. The average value of f_c , with length along the airfoil, is about 7 percent higher than that if u_m is evaluated from equation (12).

Figure 10 reveals the predicted values of the heat loss from an NACA 23012 airfoil for a difference of $70^\circ F$ between the temperatures of the fluid and of the surface at velocities ranging from 150 to 300 miles per hour. The magnitude of the weight density γ was evaluated at atmospheric pressure and at $0^\circ F$, which is the arithmetic average of the temperatures of the free stream and of the airfoil surface. The values of u_m were calculated from equation (12).

For the case of an actual tapered wing, the value q/b should be computed for each foot of span because of the variation in profile and chord length. The total rate of heat transfer would then be the sum of these q/b contributions.

CONCLUSIONS

1. The variation of the unit thermal conductance along a wing can be estimated fairly accurately by an approximate method from known heat-transfer data on smooth cylinders and flat plates.

2. An exact computation of the distribution of the unit conductance along a wing requires the determination of the position of the transition of the boundary layer from laminar to turbulent flow. Such knowledge is necessary for the proper design of the heat-distribution system in the leading edge.

3. A precise agreement between the predicted results and experimental data taken on small airfoil models is not to be expected because the transition point may occur over a large percentage of the chord in the case of models, depending on the conditions of flow; but this change in position comprises a small part of the chord in the case of full-size wings.

4. The method proposed herein is satisfactory, however, for a conservative estimate of the thermal capacity of a de-icing system. The accuracy of the method is greater for high velocities and for heating sections that extend over a larger part of the profile. The velocity along the airfoil can be obtained from static-pressure measurements or, if these data are not available, can be estimated from an equation given herein.

University of California,
Berkeley, Calif.

REFERENCES

1. Goldstein, S.: Modern Developments in Fluid Dynamics. Clarendon Press (Oxford), 1938, vol I, p. 326; vol II, pp. 366, 367, and 632.
2. Schmidt, E., and Wenner, K.: Wärmeabgabe über den Umfang eines angeblasenen geheizten Zylinders. Forschung auf dem Gebiete des Ingenieurwesens, ed. B, Bd. 12, Heft 2, March-April 1941, pp. 65-73.
3. Colburn, Allan P.: A Method of Correlating Forced Convection Heat Transfer Data and a Comparison with Fluid Friction. Trans. Am. Inst. Chem. Eng., vol. XXIX, 1935, pp. 174-210.
4. Martinelli, R. C., Tribus, M., and Boelter, L. M. K.: An Investigation of Aircraft Heaters. I - Elementary Heat Transfer Considerations in an Airplane. NACA A.R.R., Oct. 1942.
5. Seibert, Otto: Heat Transfer of Airfoils and Plates. T.M. No. 1044, NACA, 1943, pp. 15-17.
6. Martinelli, R. C., Weinberg, E. B., Morrin, E. H., and Boelter, L. M. K.: An Investigation of Aircraft Heaters. IV. - Measured and Predicted Performance of Longitudinally Finned Tubes. NACA A.R.R., Oct. 1942.
7. Bryant, L. W., Over, E., Halliday, A. S., and Falkner, V. M.: On the Convection of Heat from the Surface of an Aerofoil in a Wind Current. R. & M. No. 1163, British A.R.C., 1928.
8. Harris, R. G., Caygill, L. E., and Fairthorne, R. A.: Wind Tunnel Experiments on Steam Condensing Radiators. R. & M. No. 1326, British A.R.C., 1930.
9. Theodorsen, Theodore, and Clay, William C.: Ice Prevention on Aircraft by Means of Engine Exhaust Heat and a Technical Study of Heat Transmission from a Clark Y Airfoil. Rep. No. 403, NACA, 1931.
10. Seibert, Otto: Messungen über die Wärmeabgabe eines Profiles. Jahrb. 1938 der deutschen Luftfahrtforschung, R. Oldenbourg (Munich), p. II 224.

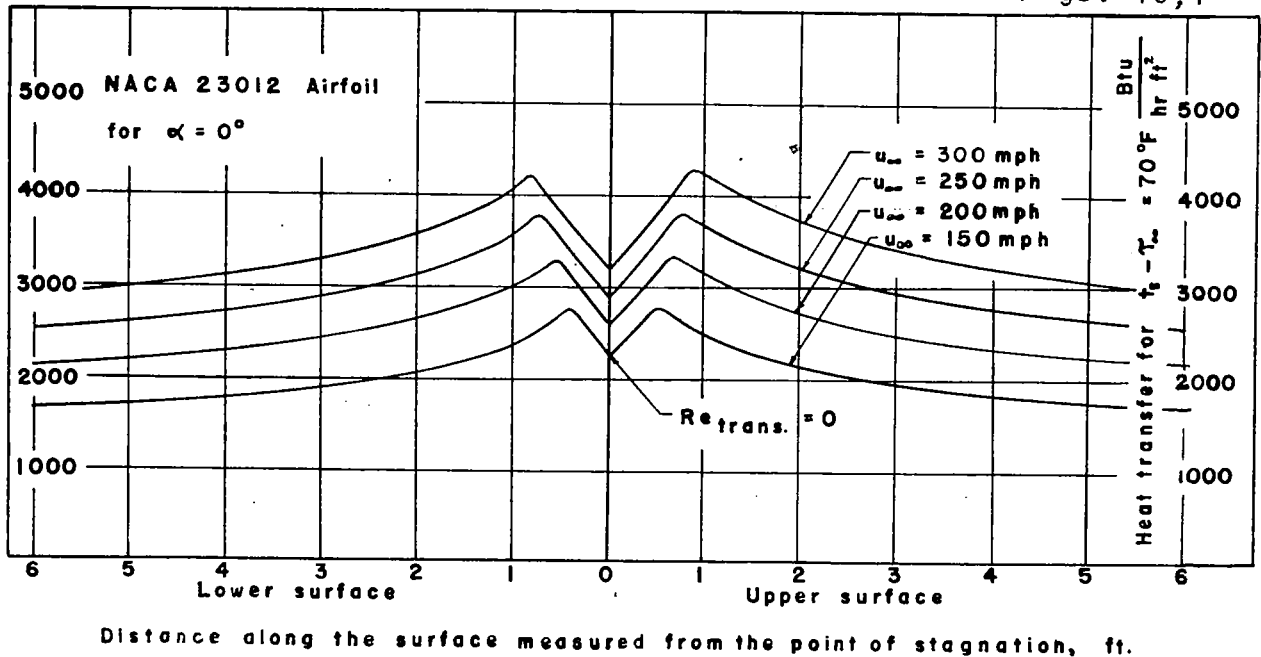
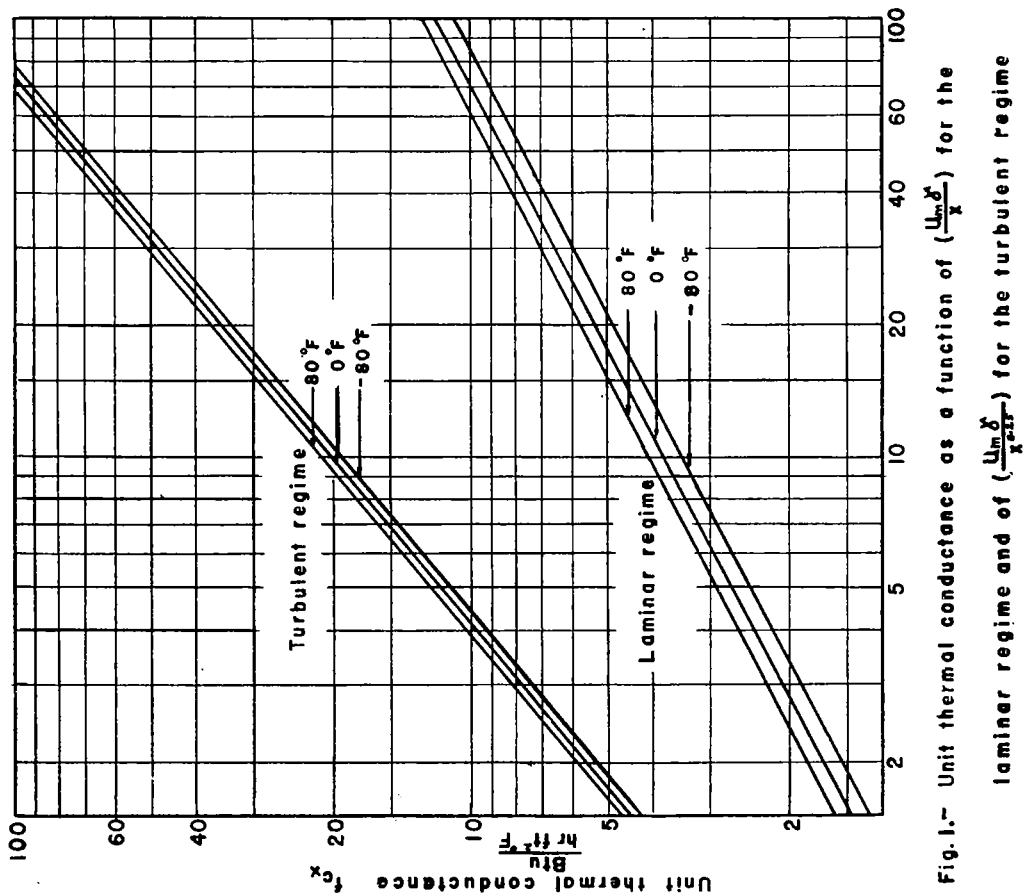


Fig.10- Predicted rate of heat transfer as a function of distance along the airfoil surface



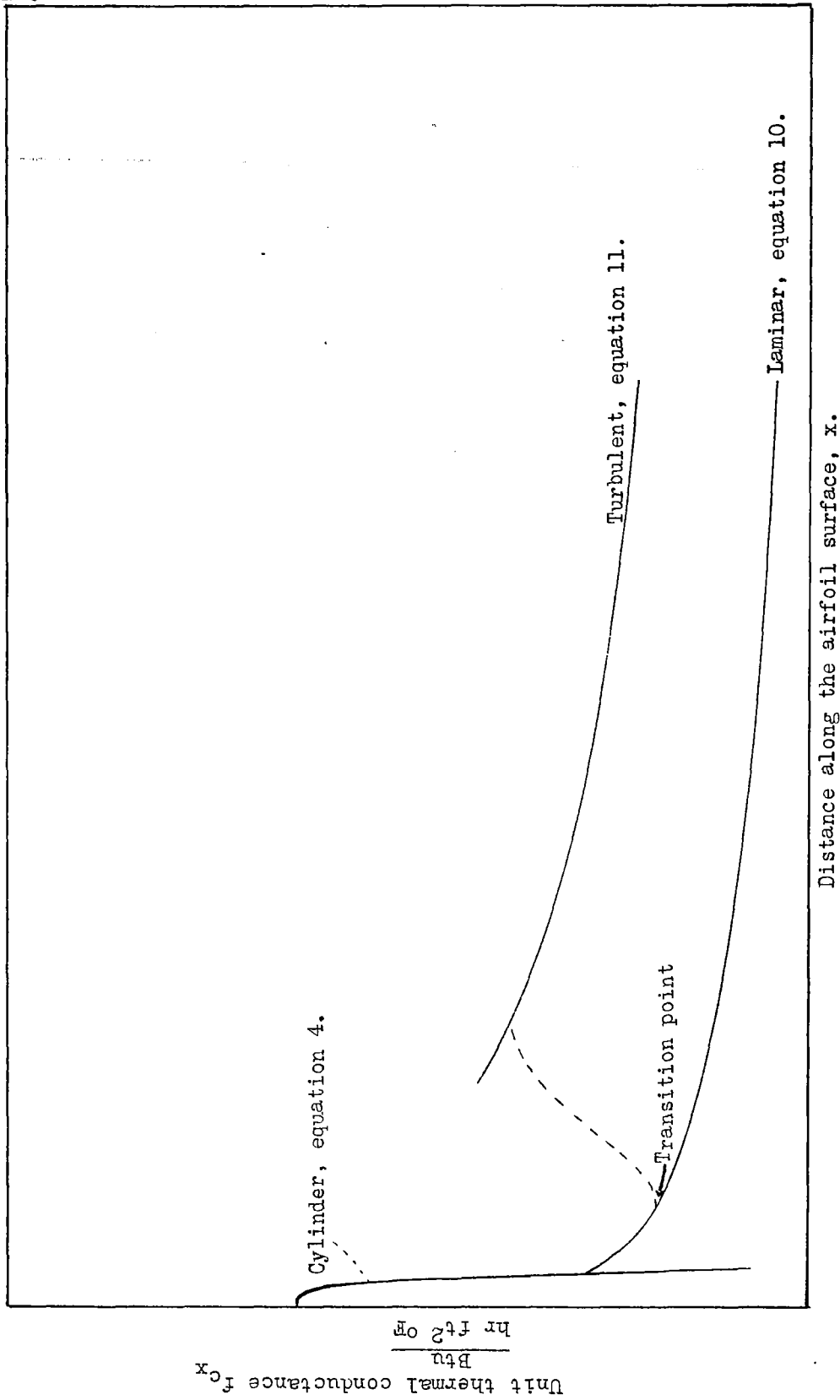


Figure 2.- Typical predicted distribution of the unit thermal conductance.



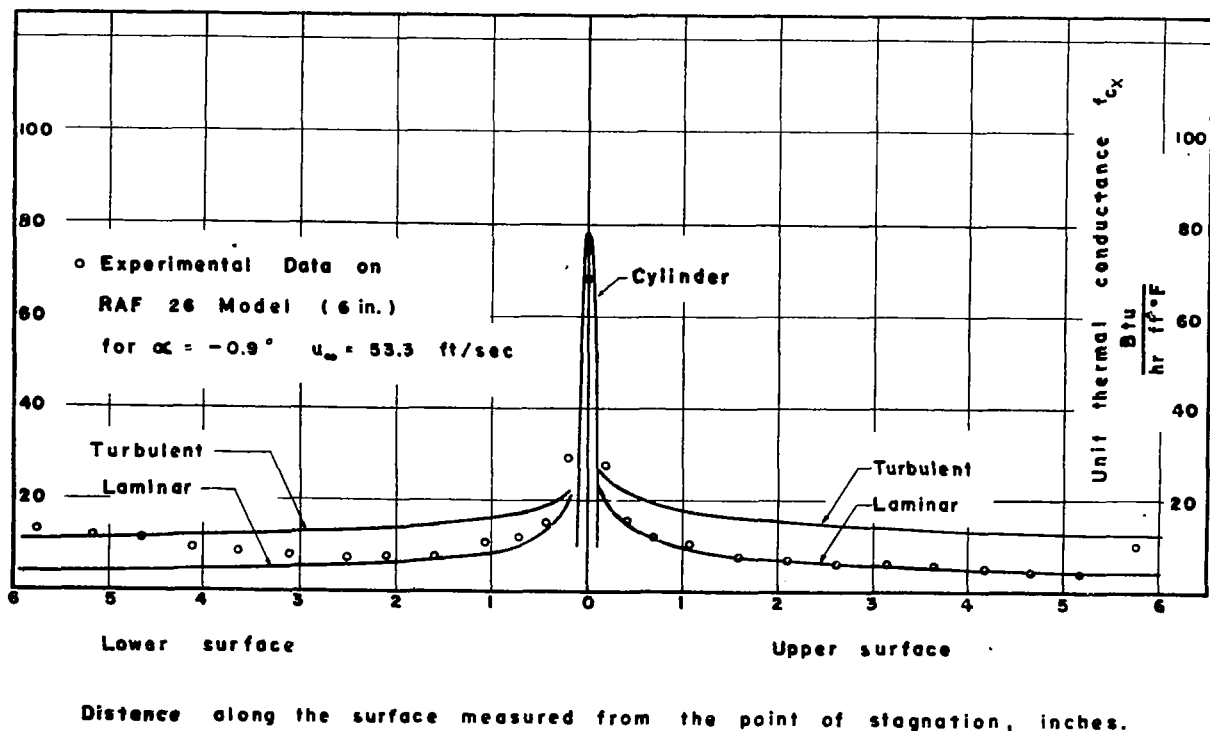
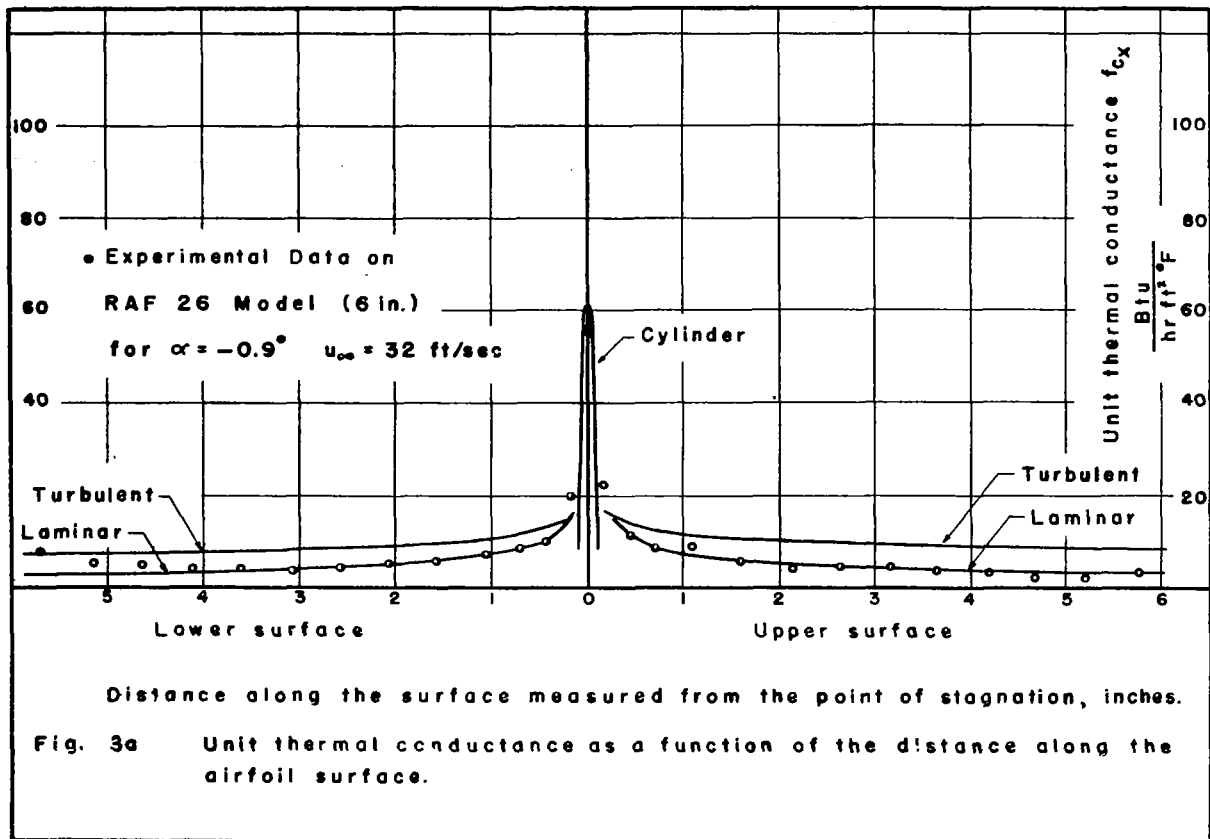


Fig. 3b Unit thermal conductance as a function of the distance along the airfoil surface.

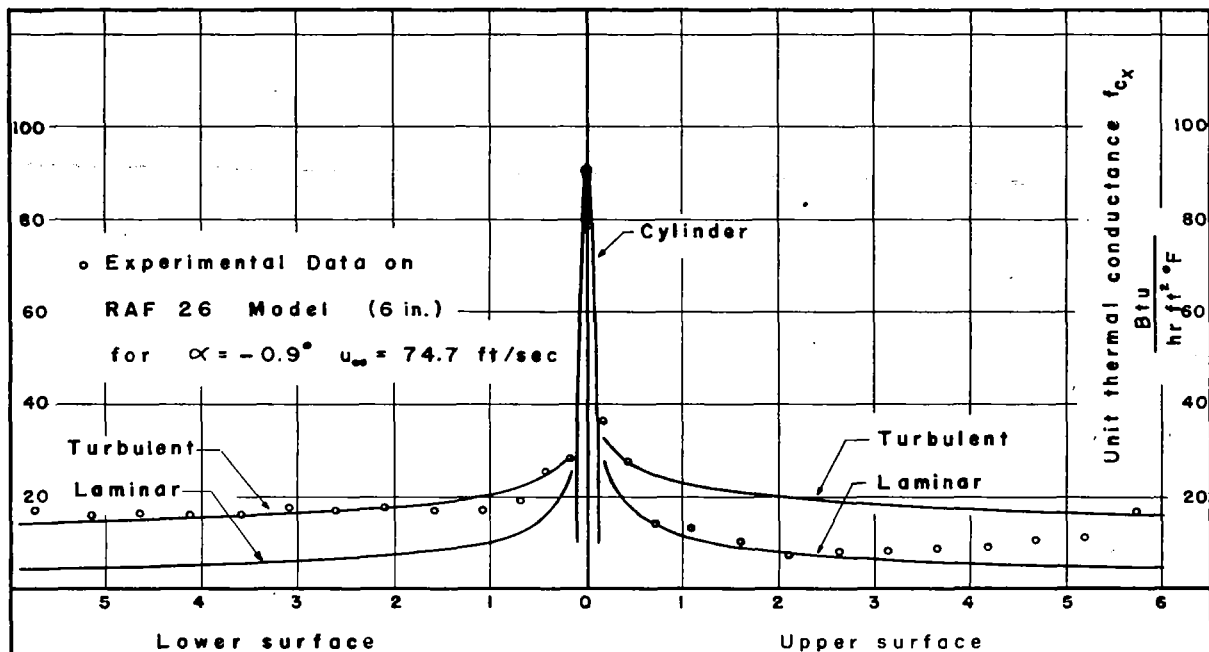


Fig. 3c Unit thermal conductance as a function of the distance along the airfoil surface.

(1 block = 10/20")

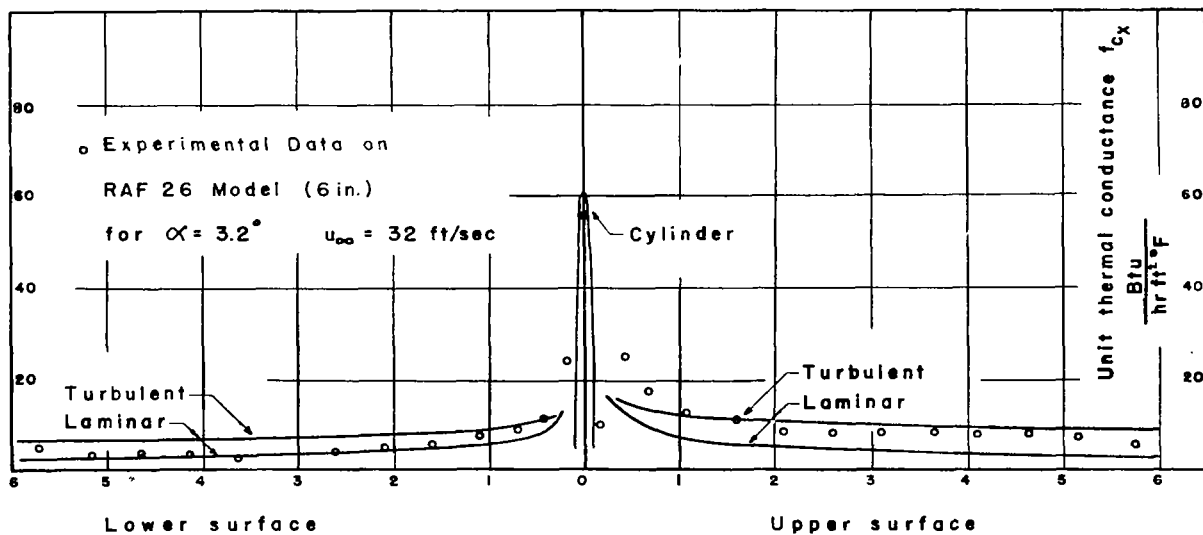


Fig. 4a Unit thermal conductance as a function of the distance along the airfoil surface.

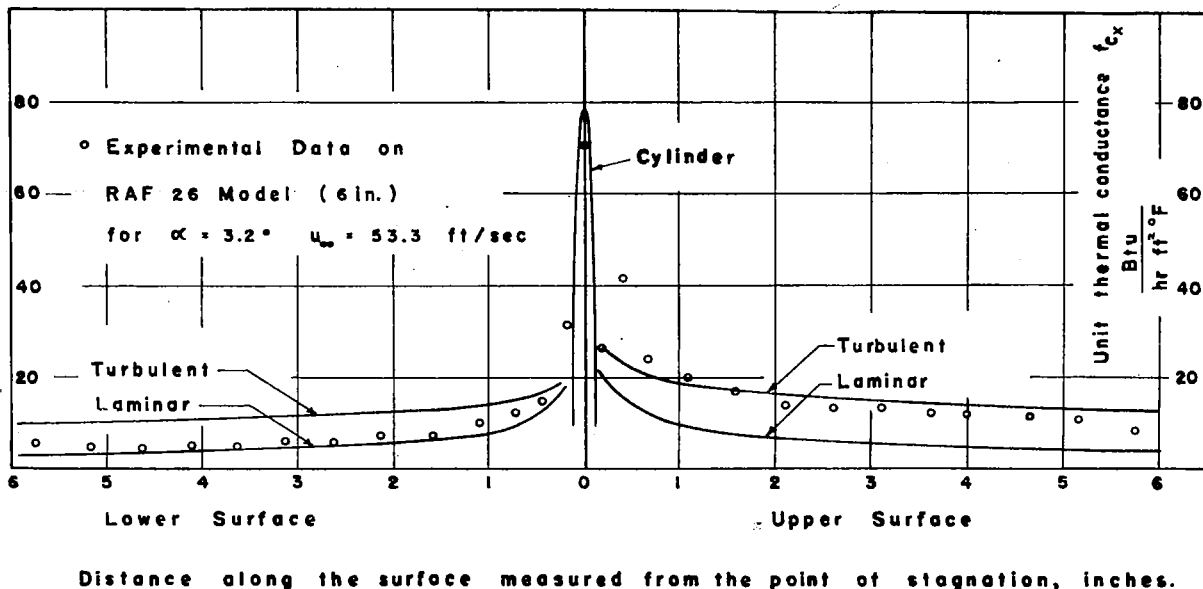


Fig. 4b Unit thermal conductance as a function of distance along the airfoil surface.

(1 block = 10/20")

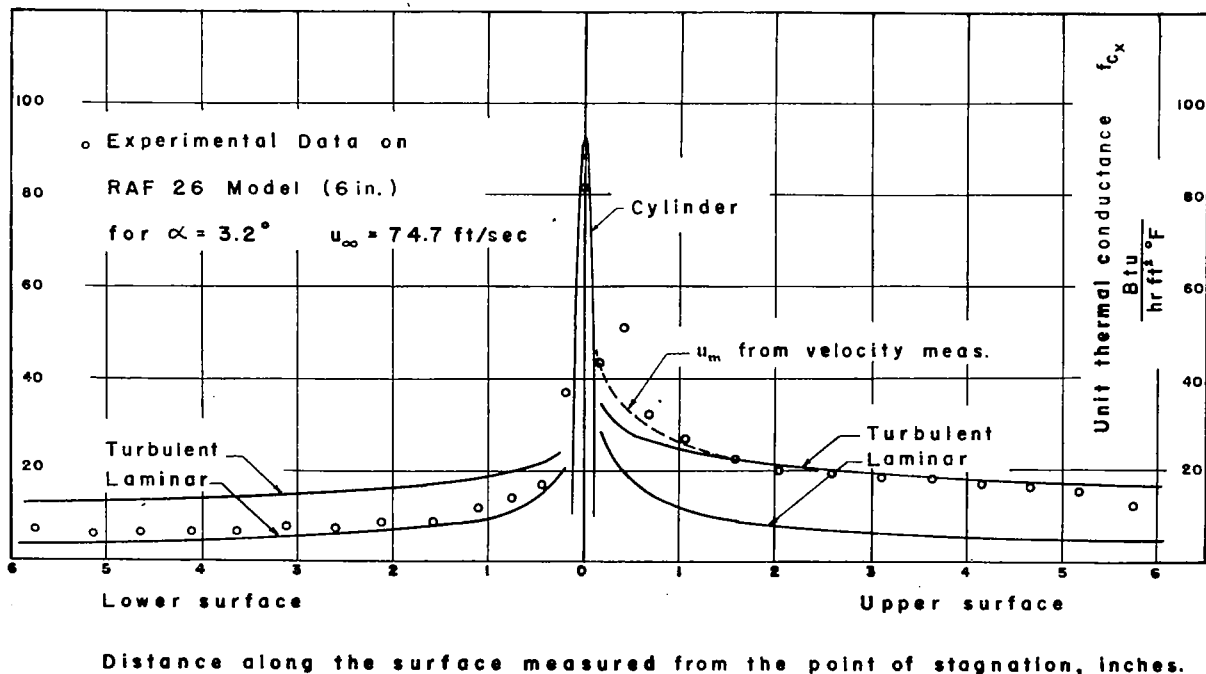


Fig. 4c Unit thermal conductance as a function of the distance along the airfoil surface.

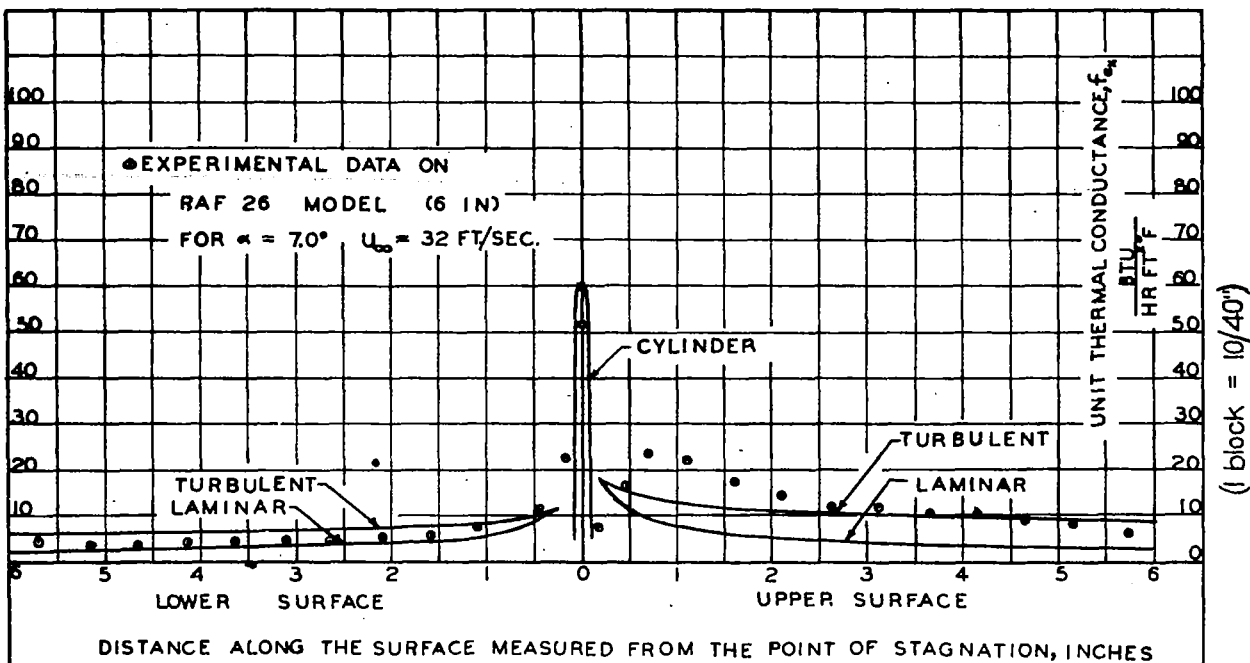


FIG. 5a UNIT THERMAL CONDUCTANCE AS A FUNCTION OF THE DISTANCE ALONG THE AIRFOIL SURFACE.

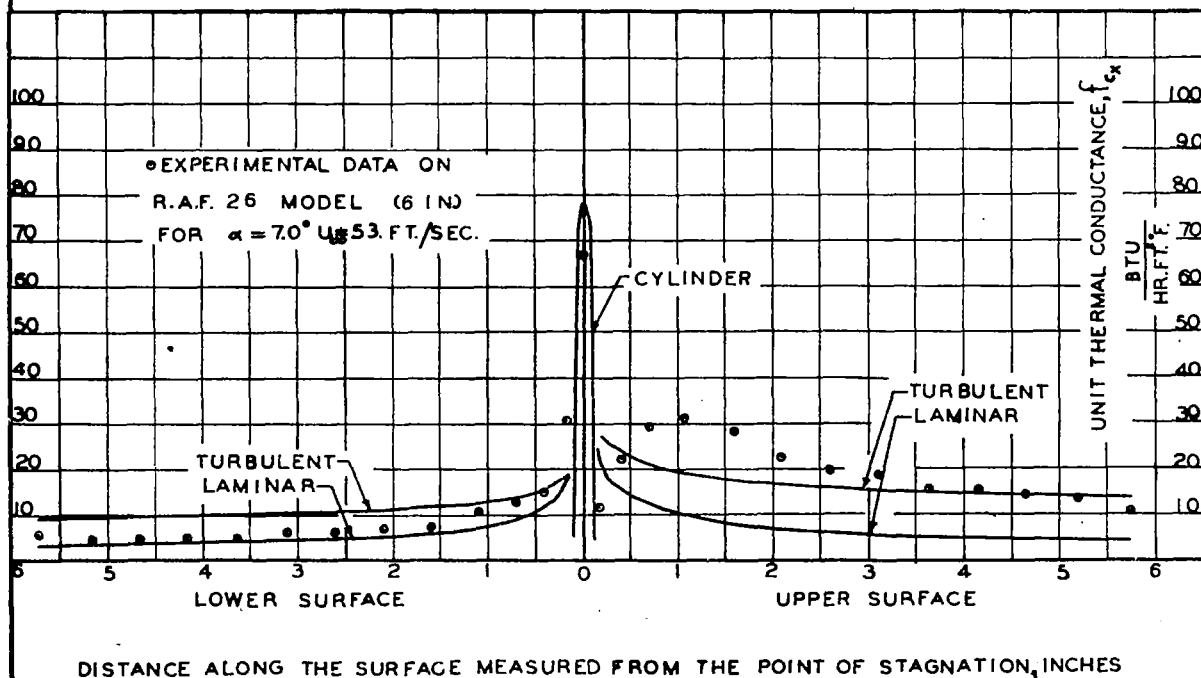
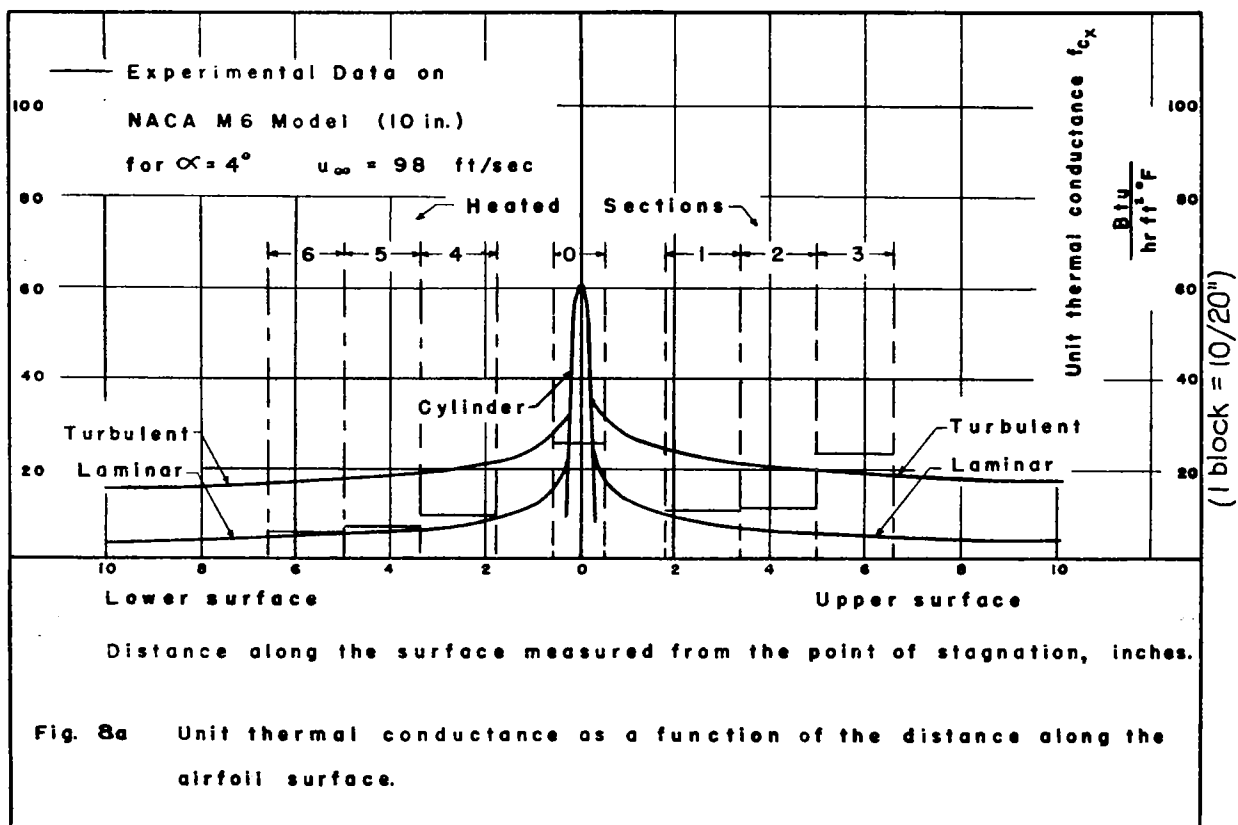
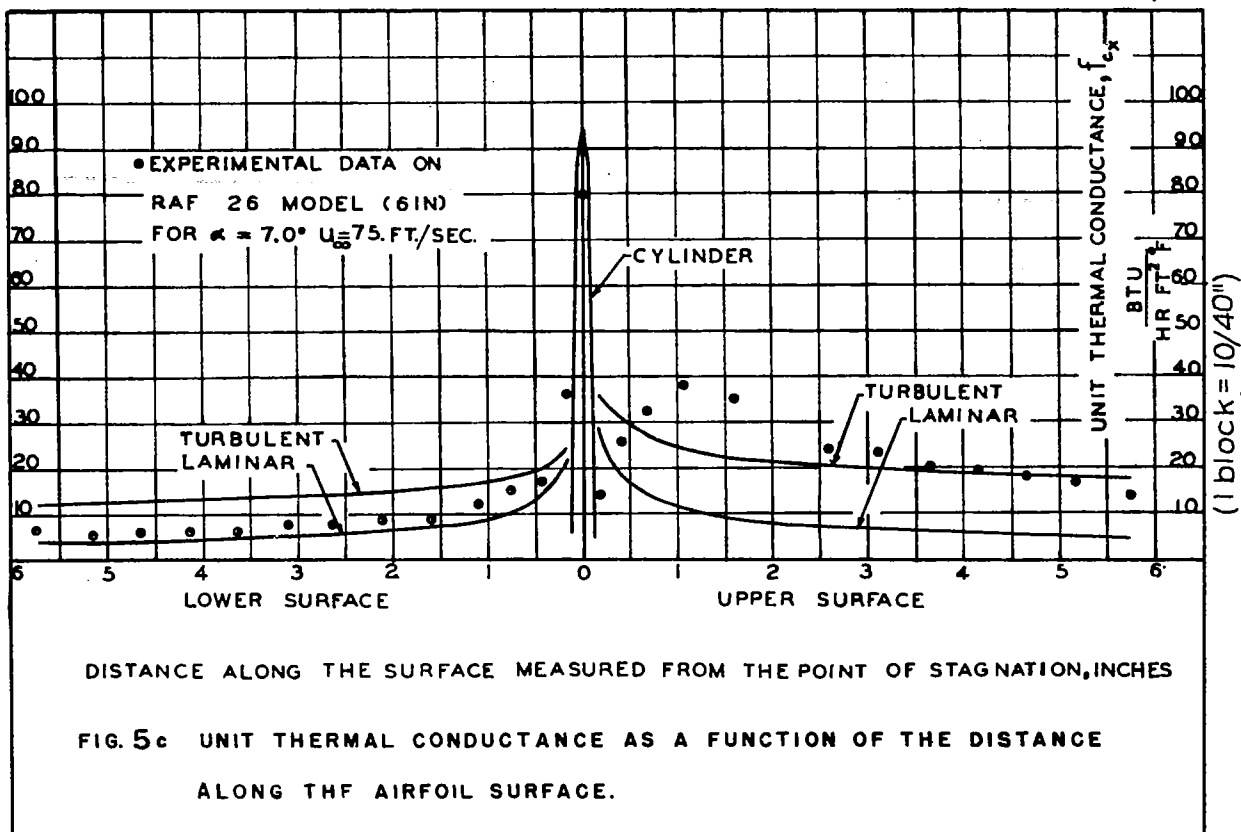


FIG. 5b UNIT THERMAL CONDUCTANCE AS A FUNCTION OF THE DISTANCE ALONG THE AIRFOIL SURFACE.



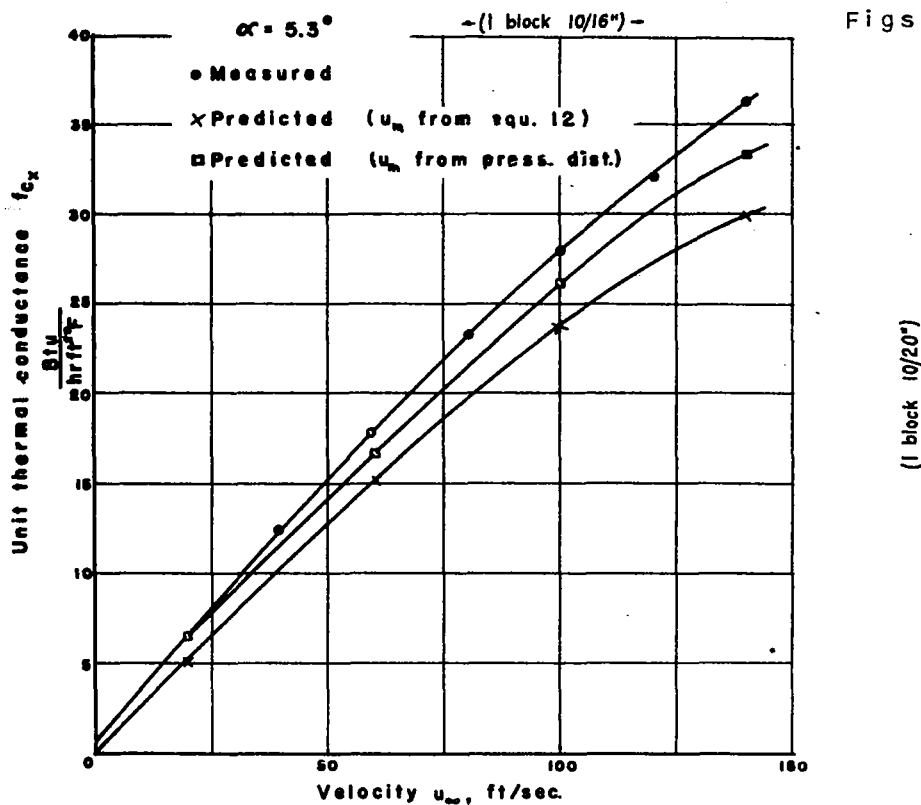


Fig. 6 Predicted and measured average unit thermal conductance of RAF 30 Airfoil as a function of velocity.

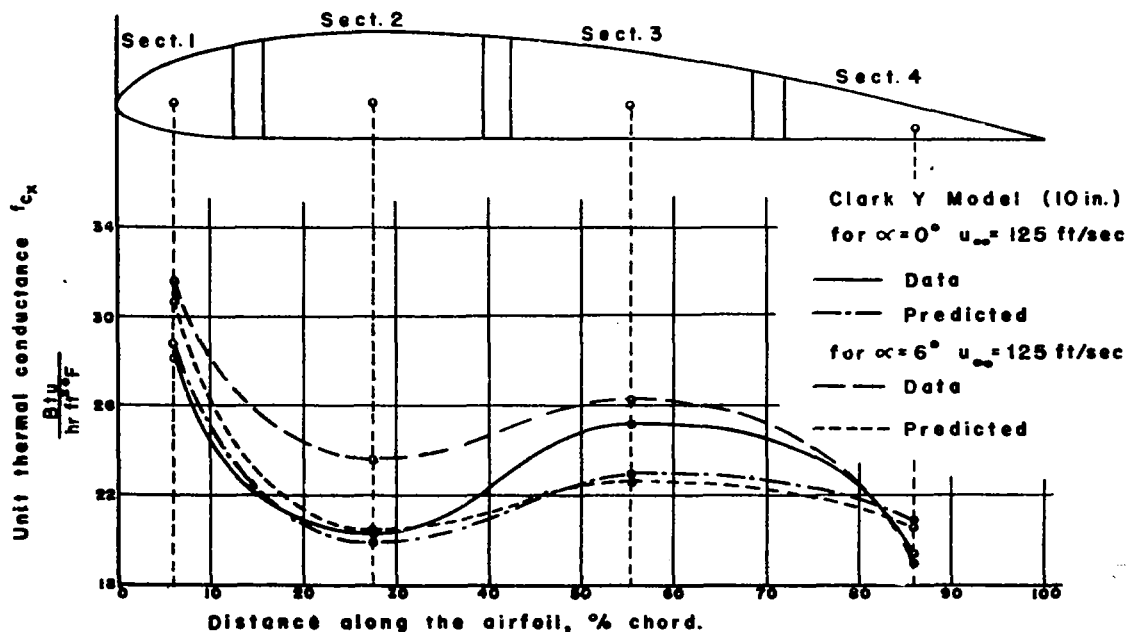


Fig. 7 Unit thermal conductance as a function of the distance along the airfoil surface.

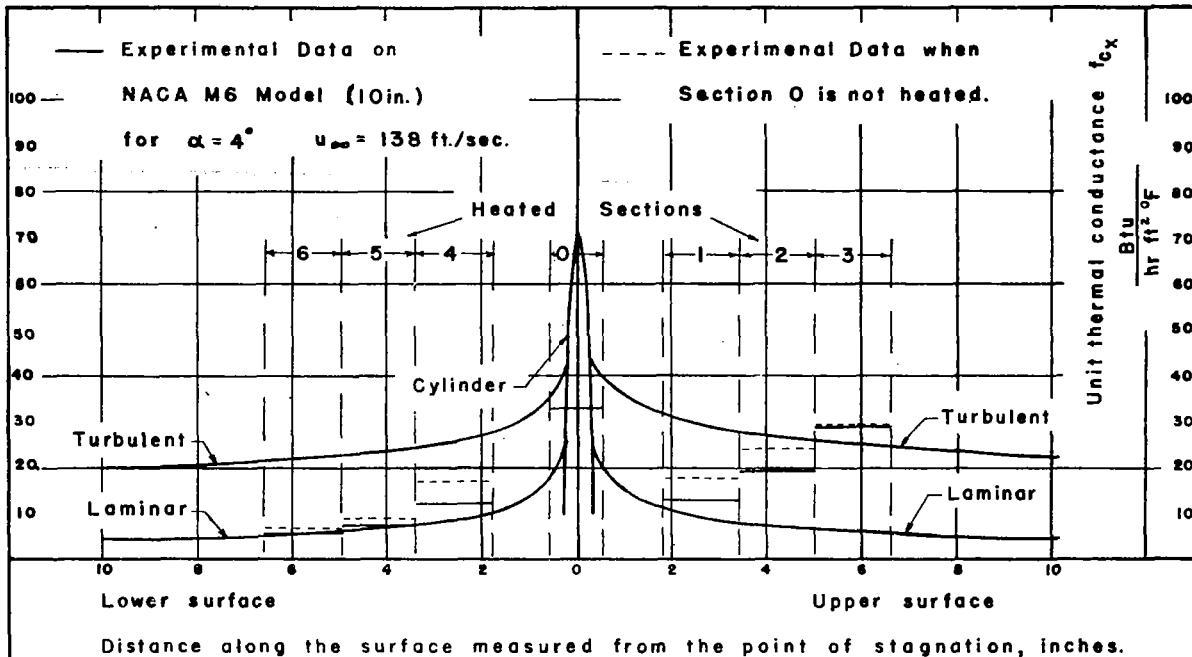


Fig. 8b Unit thermal conductance as a function of the distance along the airfoil surface.

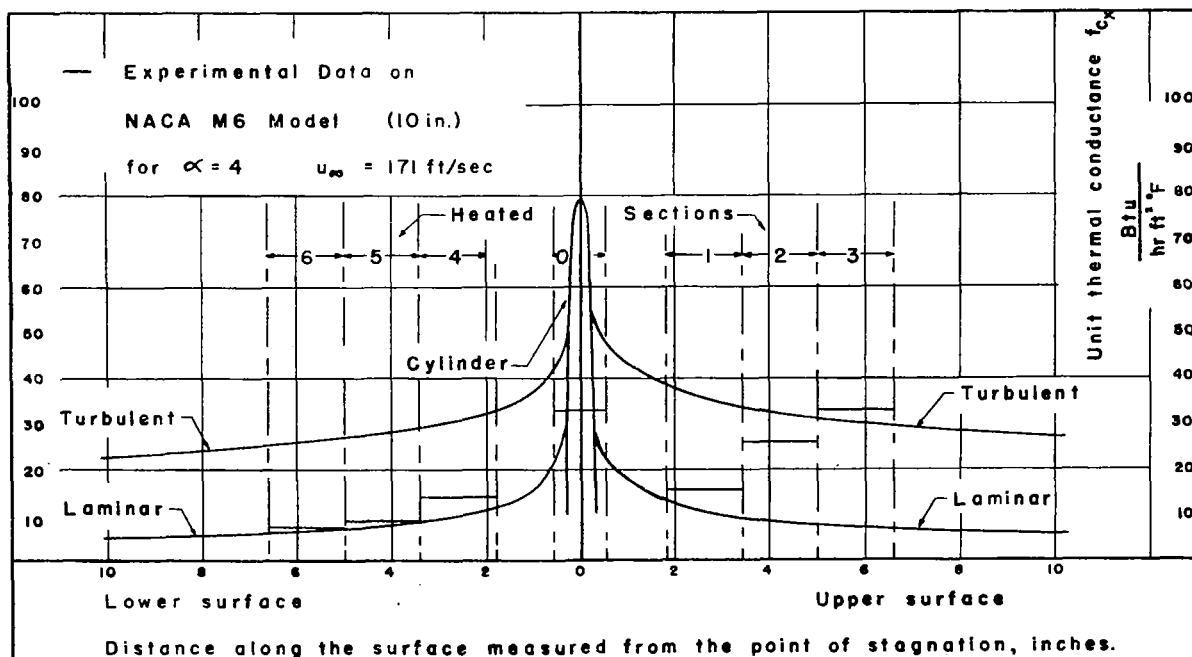


Fig. 8c Unit thermal conductance as a function of the distance along the airfoil surface.

(1 block = 10/20")

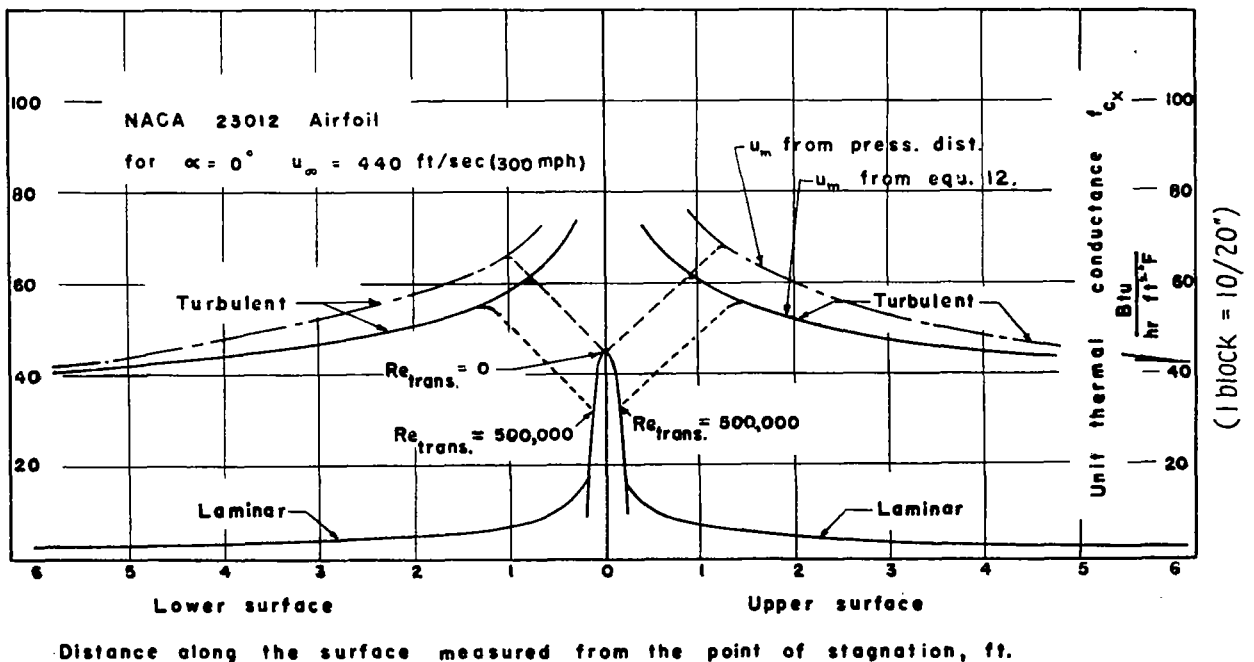
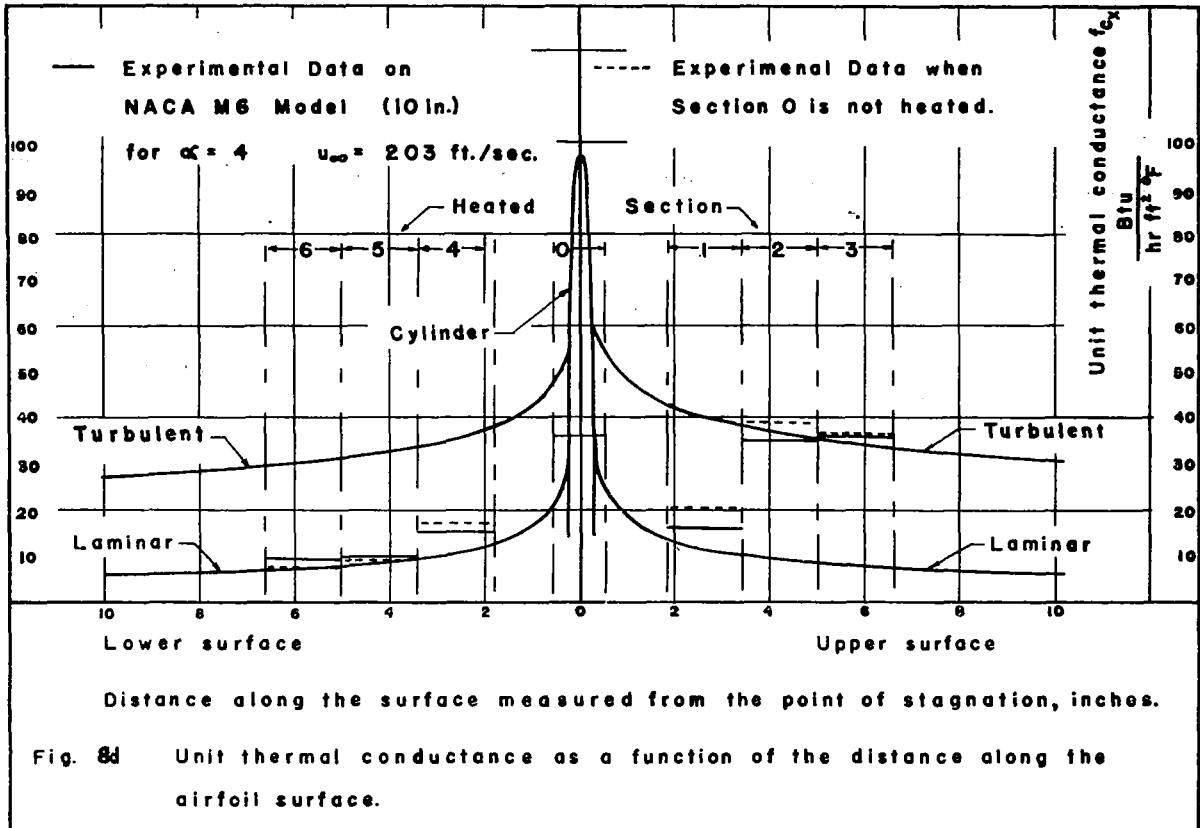


Fig. 9.— Predicted unit thermal conductance as a function of the distance along the airfoil surface.



LANGLEY RESEARCH CENTER



3 1176 01354 4466